Relationship between Edge Magnetic Field and Rotation of the Spatial Structure of Visible Light Emitted from Low Aspect RFP Plasmas on RELAX*)

Akio SANPEI, Haruhiko HIMURA, Takeru INOUE, Shinichiro INAGAKI, Natsuki KOJIMA, Ryota TAKAOKA and Takahiro SASAKI

Department of Electronics, Kyoto Institute of Technology, Matsugasaki, Sakyo Ward, Kyoto 606-8585, Japan

(Received 9 January 2023 / Accepted 3 March 2023)

The relationship between the edge toroidal field B_t and the rotation of the spatial structure of visible light emitted from reversed field pinch (RFP) plasmas is reported. The rotation of the spatial structure of visible light is captured by a high-speed camera attached to a horizontal viewing port of the RELAX , which was designed for RFP experiments. It is found that the rotation velocity and the direction of the spatial structure of visible light depend on B_t. In the non-reversal case, the structure rotates in the co-current direction, while in the counter-current direction in the reversal case. The frequency and direction of the spatial structure of visible light are consistent with magnetic fluctuations measured by magnetic probes.

Keywords: reversed field pinch, low aspect ratio, plasma rotation, high-speed camera

DOI: 10.1585/pfr.18.2402024

1. Introduction

In magnetically-confined plasmas, plasma rotations and their shear are essential in forming and sustaining a transport barrier [1–3]. In reversed field pinch (RFP) plasmas [4], spontaneous zonal flow in the plasma edge was reported [5]. Moreover, from the perspective of transition to three-dimensional (3-D) helical structure [6], a correlation between plasma flow with the phase velocity of magnetic fluctuation was investigated with ion Doppler spectrometer (IDS) to measure the velocity of impurity ions [7,8]. As of this moment, methods to control plasma flow have been explored. Improvement of the particle confinement time due to the $\boldsymbol{E} \times \boldsymbol{B}$ shear flow was investigated on MST with a method of a plasma biasing [9]. In addition, IDS measurements indicated the switching of the direction of plasma flow with changing the polarity of the toroidal magnetic field B_t at the core [10]. However, the relationship between the edge magnetic field and the plasma flow has yet to be investigated.

Measuring visible light radiation captured by a high-speed camera is a valuable passive method for measuring the plasma flow. In experiments, a high-speed camera revealed a rotating helix spatial structure in the visible light image [11–13]. Moreover, the camera diagnosed that spatial distributions of visible light corresponded to the phase of the mode of magnetic fluctuation [14].

Given the above facts, the time evolution of visible light distribution should help understand the plasma flow. In this paper, we describe results concerning the role of B_t at the plasma edge on the rotation direction of the spatial structure of visible light captured by a high-speed camera.

author's e-mail: sanpei@kit.ac.jp

*) This article is based on the presentation at the 31st International Toki Conference on Plasma and Fusion Research (ITC31).

2. Experimental Setup

All experimental data were obtained in RELAX [15], which has the major radius of $R = 0.51$ m and the minor radius of $a = 0.25$ m. Typical parameters are follows: the plasma current I_p of 50 ~ 60 kA, the electron density of 5 ~ 10 × 10^{18} m^{-3}, the electron temperature of core is 50 ~ 100 eV. The experimental setup is shown in Fig. 1. We have observed horizontal images during RFP discharges using a high-speed camera (Photron FASTCAM SA-4) with a time resolution of 100 ~ 300 kfps. A concave lens (Sigma Koki SLB-30-40N) is set in front of the horizontal viewport. Solid lines represent the limit of the visual field. Directions of I_p and B_t in the plasma core are counterclockwise viewed from the above. Magnetic probes are located at the points indicated by solid color circles, which will be referred to in Fig. 4.

3. Experimental Results About the Rotation of Visible Light Pattern

In Fig. 2, we compare the time evolutions of visible light images obtained in case of the reversal and non-reversal discharges. The time evolutions of I_p and the reversal parameter F are shown in Figs. 2 (a) and (b). Blue and red curves correspond to a non-reversal and a reversal discharge, respectively. The cross symbol in Fig. 2 (b) indicates the reversal moment for the reversal discharge.

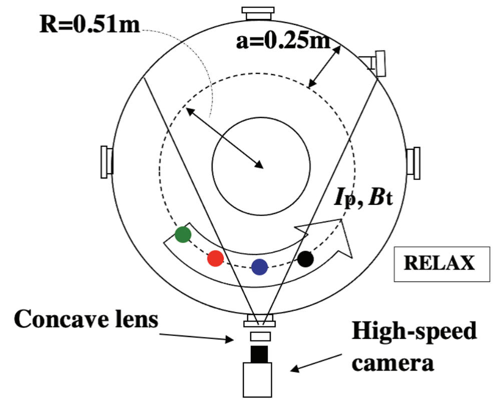

Fig. 1 Experimental setup of the installation of a fast camera onto RELAX from a horizontal port. Solid lines represent the limits of the visual field. A large open arrow indicates the direction of the plasma current I_p in the plasma core and B_t. The measurement positions of magnetic probes are indicated by closed color circles, which will be referred to in Fig. 4.

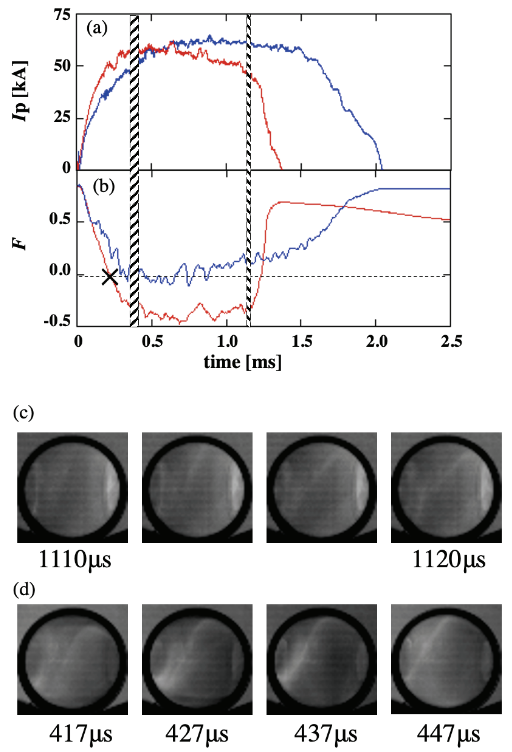

Fig. 2 Time evolution of I_p (a) and F (b) for two discharges. Blue and red lines in (a, b) correspond to a non-reversal and a reversal discharge, respectively. (c) and (d) show the time evolution of visible light images obtained from the horizontal port corresponding to the non-reversal and the reversal discharge, respectively.

Figures 2 (c) and (d) show the time evolution of visible light images obtained from the horizontal port, corresponding the non-reversal and the reversal discharge, respectively. Each time window is indicated by shaded areas in Figs. 2 (a) and (b). In both cases, a part of the visible light structure was coming into view, distributing diagonally from the bottom left to the top right. The spatial structure of the visible light had the periodicity $m = 1/n = -4$, where m is the poloidal mode number, and n is the toroidal mode number [12]. In the non-reversal discharge, images are shown from 1110 μs to 1120 μs after plasma ignition, and F is approximately 0.15. As shown in Fig. 2 (c), the helical structure moves to a co-current direction with a phase velocity of approximately 6.3×10^4 rad/s corresponding to 3.9×10^3 m/s under the assumption that it locates on the surface of the wall. On the other hand, in the reversal discharge, images are shown from 417 μs to 447 μs, and F is approximately -0.35 as seen in Fig. 2 (d). The helical structure moves to the counter-current direction with a phase velocity of approximately 4.0×10^4 rad/s corresponding to 2.5×10^3 m/s under the same assumption. The experimental results clearly show that the change in the direction of rotation of the helical structure corresponds to reversal or non-reversal discharges.

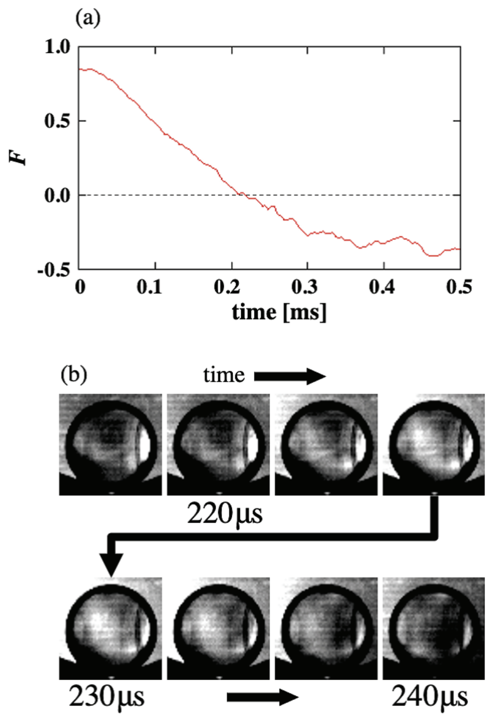

Fig. 3 Time evolutions of F (a) and 2D visible light image (b) at the initial phase of reversal discharge corresponding to the red line in Fig. 2.

Figure 3 shows the behavior of helical visible light structure on the initial phase of reversal discharge, corresponding to the data by red in Fig. 2. Time evolutions of F and the 2D visible light image are shown in Figs. 3 (a) and (b), respectively. One notes that Fig. 3 (a) is the enlarged time window around a reversal moment indicated by the cross symbol in Fig. 2 (b). The edge B_t is switched from positive to negative at 220 μs, as shown in Fig. 3 (a). In Fig. 3 (b), a part of the helical structure comes into view, distributing diagonally from the top left to the bottom right.

The difference in the appearance of visible light structures between Fig. 2 and Fig. 3 corresponds to the difference in the phase of the helical structure. These snapshots show the switching of the direction of rotation of the helical structure from the co-current direction to the counter-current direction at approximately 230 μs, i.e., just after the edge B_t reversal.

Figure 4 (a) shows the spatially resolved B_t fluctuations of non-reversal discharge, corresponding to the blue curve in Fig. 2. These signals are measured by toroidally separated magnetic probes at the top of each $\pi/8$ whose colors correspond to Fig. 1. The signals indicate that the fluctuations propagate toroidally with a frequency of ~ 10 kHz. The direction of propagation is the co-current direction, which is consistent with that of the helical visible light. Figure 4 (b) shows the time evolution of B_t fluctuations obtained with probes located top and bottom of the blue symbol in Fig. 1. The signals show opposite phases with each other and provide odd m modes. Moreover, observed visible light patterns are superimposed as square symbols with a slash. Blue squares with a slash from the bottom left to the top right correspond to the pattern Fig. 2, and the red symbols correspond to the pattern Fig. 3. It is recognized that the helical structure relates with the magnetic fluctuation. The frequency and direction of propagation of the magnetic fluctuation are the same as those of the helical visible light structure.

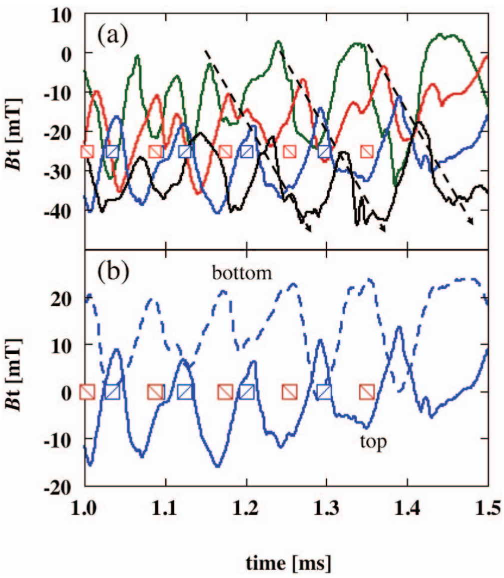

Fig. 4 Time evolution of the edge B_t. (a) Four signals were obtained with toroidally separated magnetic probes located at the top. (b) Two signals were obtained with probes located top and bottom of the blue symbol. Square symbols indicate the phase of the visible helical image.

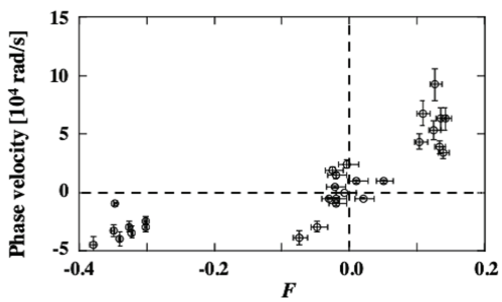

Fig. 5 Rotation velocity is plotted as a function of F. The rotation velocity shows an increasing trend with the increase of F. The direction of toroidal rotation changes as the sign of F changes.

According to the results in Fig. 4, we can estimate the phase velocity of rotation of helical visible light from measured images. Figure 5 shows the dependence of the rotation direction of helical visible light on F. Each data is obtained from a different discharge with I_p ~ 60 kA. The rotation velocity and direction depend on the edge B_t. In non-reversal discharge, the helical structure rotates in the co-current direction. In reversal discharge, on the other hand, the helical structure rotates in the counter-current direction. It is found that the rotation speed in reversal cases is slower than that of non-reversal cases.

4. Discussion

In experimental observations, a correlation between fluctuation and flow exists, while rotation of the spatial structure of visible light depends on the edge B_t. A plausible reason for those observations is that the plasma rotation is caused by $\boldsymbol{E} \times \boldsymbol{B}$ drift. Figure 6 shows a schematic of the hypothesis for the rotation of the spatial structure of visible light. A spatial profile of visible light with a phase corresponding to the pattern Fig. 3 is described by a point blank line, which is labeled as A. An outward radial electric field E_r exists at the plasma periphery because of the potential difference between the finite plasma space potential and the vacuum wall that is grounded. Moreover, the poloidal magnetic field B_p is produced whenever I_p flows mainly in the toroidal direction in plasma. The total magnetic field $\boldsymbol{B}$

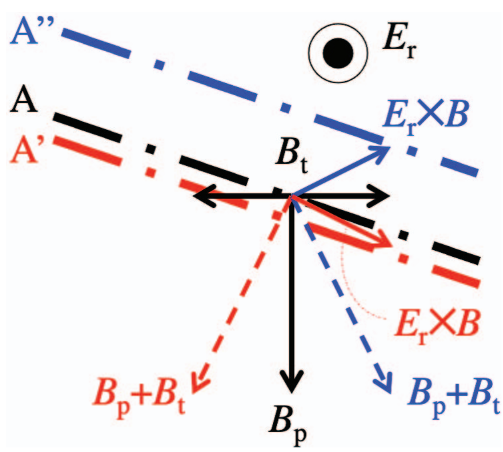

Fig. 6 Schematic of hypothesis due to $\boldsymbol{E} \times \boldsymbol{B}$. The red and blue symbols correspond to negative and positive F.

is thus expressed by $B_p + B_t$, which is indicated by the colored dashed arrows. The color of the arrows corresponds to the edge's direction of B_t. Therefore, the direction of $E_r \times \boldsymbol{B}$ is indicated by the solid colored arrows. When F is negative, the point blank line moves to the right lower direction along the red $E_r \times \boldsymbol{B}$ arrow. Subsequently, the point-blank line moves from A to A' (red one), which means it has moved from the right- to the left-hand side. On the other hand, when F is positive, the point-blank line moves from A to A" (blue one). This means that the point-blank line moves in the opposite direction, from the left- to the right-hand side. Data show that the helical visible light structure moves to the left- or the right-hand side, depending on the edge B_t.

5. Summary

The relationship between the edge B_t and the rotation of the spatial structure of visible light was investigated. Rotations of the spatial structure of visible light were captured by a high-speed camera in RFP experiments on RELAX. In the non-reversal case, the helical structure rotates in the co-current direction, while in the counter-current direction in the reversal case. The rotation velocity and direction of the helical visible light structure seem to correlate with the edge B_t. Magnetic probes indicate that the frequency and the direction of magnetic fluctuations are consistent with those of helical visible light structure. These results strongly suggest that a $\boldsymbol{E} \times \boldsymbol{B}$ plasma flow should be related to the spatial structure of visible light. This will be double-checked by using complex probes constituted with magnetic, capacitive, and mach probes to measure $\boldsymbol{B}$, $\boldsymbol{E}$, and the ion flow $\boldsymbol{V}$ simultaneously. In addition, we will install an IDS measurement to establish the relationship between $\boldsymbol{V}$ and the spatial structure of visible light.

One of the authors (A. S.) thanks Prof. S. Masamune, Prof. S. Ohdachi, Dr. Y. Narushima, Dr. K. Yambe, and Dr. K. McCollam for their fruitful comments on this study. This work is partially supported by JSPS KAKENHI Grant 20KK0063 and 21H01056 and the National Institute for Fusion Science Grant NIFS22KIPP016 and NIFS20KOAP035, and, in part, by the Joint Usage/Research Program on Zero-Emission Energy Research, Institute of Advanced Energy, Kyoto University ZE2022A-24.

[1] K. Ida, Phys. Fluids B **4**, 2552 (1992).
[2] Y. Sakamoto, Y. Kamada, S. Ide, T. Fujita, H. Shirai, T. Takizuka, Y. Koide, T. Fukuda, T. Oikawa, T. Suzuki, K. Shinohara, R. Yoshino and JT-60 Team, Nucl. Fusion **41**, 865 (2001).
[3] K. Ida, M. Yoshinuma, H. Tsuchiya, T. Kobayashi, C. Suzuki, M. Yokoyama, A. Shimizu, K. Nagaoka, S. Inagaki, K. Itoh and the LHD Experiment Group, Nat. Phys. **6**, 5816 (2015).
[4] L. Marrelli, P. Martin, M.E. Puiatti, J.S. Sarff, B.E. Chapman, J.R. Drake, D.F. Escande and S. Masamune, Nucl. Fusion **61**, 023001 (2021).
[5] T. Nishizawa, A.F. Almagri, J.K. Anderson, W. Goodman, M.J. Pueschel, M.D. Nornberg, S. Ohshima, J.S. Sarff, P.W. Terry and Z.R. Williams, Phys. Rev. Lett. **122**, 105001 (2019).
[6] R. Lorenzini, E. Martines, P. Piovesan, D. Terranova, P. Zanca, M. Zuin, A. Alfier, D. Bonfiglio, F. Bonomo, A. Canton, S. Cappello, L. Carraro, R. Cavazzana, D.F. Escande, A. Fassina, P. Franz, M. Gobbin, P. Innocente, L. Marrelli, R. Pasqualotto, M.E. Puiatti, M. Spolaore, M. Valisa, N. Vianello, P. Martin, RFX-mod team and collaborators, Nat. Phys. **5**, 570 (2009).
[7] J.S. Sarff *et al.*, Proceedings of the 23rd IAEA Fusion Energy Conference, Daejon, OV/5-3Rb. IAEA, Vienna, (2010).
[8] F. Bonomo *et al.*, Nucl. Fusion **51**, 123007 (2011).
[9] D. Craig, A.F. Almagri, J.K. Anderson, J.T. Chapman, C.-S. Chiang, N.A. Crocker, D.J. Den Hartog, G. Fiksel, S.C. Prager, J.S. Sarff and M.R. Stoneking, Phys. Rev. Lett. **79**, 1865 (1997).
[10] H. Arimoto, K.I. Sato, A. Nagata, S. Masamune, Y. Aso, K. Ogawa, S. Yamada, A. Matsuoka and H. Oshiyama, Nucl. Fusion **27**, 1021 (1987).
[11] T. Onchi, N. Nishino, R. Ikezoe, A. Sanpei, H. Himura and S. Masamune, Plasma Fusion Res. **3**, 005 (2008).
[12] A. Sanpei, R. Ikezoe, T. Onchi, K. Oki, M. Sugihara, Y. Konishi, S. Fujita, M. Nakamura, A. Higashi, H. Motoi, H. Himura and S. Masamune, Plasma Fusion Res. **5**, S2306 (2010).
[13] T. Onchi, R. Ikezoe, K. Oki, A. Sanpei, H. Himura, S. Masamune, N. Nishino and H. Koguchi, J. Phys. Soc. Jpn. **80**, 114501 (2011).
[14] P. Scarin, M. Agostini, G. Spizzo, M. Veranda, P. Zanca and the RFX-Mod Team, Nucl. Fusion **59**, 086008 (2019).
[15] S. Masamune, A. Sanpei, R. Ikezoe, T. Onchi, K. Murata, K. Oki, H. Shimazu, T. Yamashita and H. Himura, J. Phys. Soc. Jpn. **76**, 123501 (2007).